PROCEEDINGS
JOINT CONVENTION BANDUNG (JCB) 2021
November 23rd – 25th 2021

Seismic HC Detection in Fluvio - Deltaic System Using Integrated Quantitative Interpretation by Utilizing Reprocessing Data: Case Study of Intan Field, TAF - Asri Basin, Offshore SE Sumatera

Pranowo Nugroho[1], Hairunnisa[1], Dwandari Ralanarko[1]

[1]Pertamina Hulu Energi OSES

Abstract

Along with the development of seismic imaging and increasingly advanced computing technology, the dream of geoscientists to identify reservoir fluids from seismic data will be easier to be accurately and comprehensively conduct. The need for complex seismic data in quality and quantity is a challenge in itself as an initial step for static and dynamic studies to determine how much oil reserves remain. Seismic processing technology and new quantitative seismic methods will further assist in an old oil fairway and mature field such as Fluvio-Deltaic Depositional Environment of Intan Field, Asri Basin, Offshore SE Sumatra. The results of seismic reprocessing show that the quality and quantity of new seismic data have increased sharply compared to old seismic data. This reprocessing data has been using to identify hydrocarbon reservoirs with various quantitative seismic methods. The results of the seismic attribute, AVO, seismic impedance (LambdaRho -VpVs Ratio), lithological impedance (LI), spectral decomposition, RGB blending, and seismic facies results using the Bayesian classification method show that seismic hydrocarbon detection in a Meandering Channel System of sandstone reservoir can be identified accurately through integrated quantitative analysis.

Introduction

Asri Basin has been described as a back-arc, half-graben rift basin (Young and Atkinson, 1993) and a basin with a composite extensional style that begun as an intra-cratonic, "sag style" basin (Aldrich et. al., 1995). Asri Basin is part of a series of Tertiary half-graben developed on the Asian continental margin that has occupied a retro-arc setting since early Neogene times. It covers an area approximately 3500 sq. km and has up to 16,000 feet of sediment ranging from Paleocene to Pleistocene in age. It is bounded to the East by N-S trending fault, downthrown to the West, while the southern margin is marked by a regional NW-SE trending wrench system. There are three major tectonic periods that affected the structural style and depositional systems in the Asri Basin: I) Rift Initiation, II) Syn-Rift, and III) post rift.

Structural control on major axial drainage systems would exert tremendous influence on sand supply to any particular basin at any given time. Basin integration and its control on axial fluvial systems is probably an important part of the story in the stratigraphy of the Asri Basin fill. (Sukanto, et al., 1998) introduce the petroleum system of the Asri Basin, Java Sea, Indonesia. The main reservoir rocks in the Asri Basin are Oligocene to early Miocene fluvial, alluvial, marginal marine, and deltaic sandstones of the Talang Akar Formation (TAF). The TAF of the Asri Basin is divided into Zelda and Gita Member. Typical composite logs of these fields show the vertically stacked sandstone reservoirs. Regional seals are provided by shales at the top of and directly above the TAF by thick mudstones of the succeeding Gumai Fm. The close interplay of the abundant fault and permeability migration pathways, high-quality reservoir, source, and seal facies in a region of high heat flow has thus handled the accumulation of large reserves of oil in the Asri Basin (Figure 01).

The Miocene Gita member of the TAF represent deposits of a post-rift fluvial system that records the northward advance of a late Oligocene to early Miocene marine transgression. Gita reservoirs sandstones is the most prolific hydrocarbon interval and therefore one of the most valuable assets in the Southeast Sumatera Block. If production continues to follow development trends for a mature basin, then the most significant reserve additions will come from exploration and the most productive intervals. One of the candidates is Intan prospect, located at the northwest flank of Asri Basin with a three-way dip structure based on the 2D seismic mapping.

In 1987, a 'final' five-well exploration programmed was undertaken to evaluate the Intan prospect. Intan-01 has prioritized drilled first. It met 76 feet of net oil pay and flow tested a cumulative 5845 BOPD, proving the Asri Basin as a majors oil-bearing area. The development of Intan Field has proposed to recover oil reserves from TAF discovered by Intan-01 well and confirmed in subsequent and appraisal drilling. Since the development of the Intan field began in 1990, near-field exploration has focused primarily on infill prospects using 3D seismic (Wight, et al., 1997).

Seismic Processing

With the success of the discovery of two giant fields in the Asri Basin, namely Intan Field and Widuri Field, the existence of 3D seismic data is an absolute prerequisite for the development program. 3D seismic is an extremely powerful delineation tool that is also cost-effective, particularly when well costs are high. The success is directly attributable to the better structural interpretation made possible by the 3-D survey (Sheriff, 1992). The greatest impact of 3-D surveys has been the ability to match platform size, several wells' slots, and production facilities to the more accurately determined field reserves.

3D seismic data at Intan field was acquired and processed in 1991. The primary lines were recorded using a single boat outfitted with a dual air-gun source and two streamers. The survey was a plan to produce 21-fold coverage on a 6.25 m CMP by 25 m line spacing. After final editing, the 3D volume formed a total of

approximately 15,000 km of 256 channel data. The recording was to 3 seconds at a sample rate of 1ms. The survey was processed using a 2ms sample rate, a record length of 3 seconds, and the nearest 240 channels. The limitations of machine computation when it happened allowed only for the production of seismic post-stack, by using velocity analysis every 500m, 2D Dip Move Out (DMO) in the first process, high-resolution radon de-multiple process has not been applying. Hardware technology and processing parameters were unable to perform processing parameters such as 3D Kirchoff Pre Stack Time Migration (PSTM), high-resolution radon de-multiple, and 5D interpolation.

However, the 1991 3D post stack seismic data with a spacing of inline 25 m, still has excellent geological interpretation results. Seismic amplitude attribute on TAF formation shows that the reservoir zone in the Intan Field can be identified clearly as a braided channel on Zelda Member and meander in Gita Member. The 30 series sand of the Intan field are found within the uppermost part of the Gita Member. The 30-1 sand categorized as meandering fluvial channel sandstones trending northwest southeast.

Processing new seismic data has been complete at the Intan Field for a total area of around 108 km^2 in 2020. The purpose of this reprocessing data is to reveal a new paradigm and provide a better-quality resolution of signal to noise ratio on the seismic data. It is necessary to improve the seismic data quality as input for the static and dynamic model study. This procedure has been designed to convert the original SEG-D raw data from the acquisition (tape format) to hard disk media as an initial step. A comparison of the new seismic flow processing steps with the previous process has shown in Table 01. Based on the processing flow, five steps have a powerful impact on the data compare to the previous one. There are 3D SRME shallow water de-multiple, Tau-Pi deconvolution, high-resolution radon de-multiple, 5D (inline, xline, offset, azimuth, and frequency) interpolation and regularization, and 3D Kirchoff PSTM.

Predictive deconvolution attenuates multiple that involve surface and near surface reflectors. It can remove reverberation or ringing caused by the water layer. The predictive deconvolution predicts a lag (gap) that is equal to the first or second zero crossing. In this study we set 320ms operator length and 16ms gap test for the best Tau-Pi deconvolution parameter. The radon demultiple method is a method for reducing long period multiples mixed with data. The input data has been corrected by NMO, the primary event will be flat (to Zero Offset), while the multiple events is still in a downward and upward curve from the primary data. This happens because the multiple velocities are smaller than the primary velocities at the same depth. Prior to running PSTM, 5D regularization and interpolation should be run to optimize the migration result. 5D interpolation uses a neighborhood of acquired seismic data to predict the missing data. Ideally, data that are missing in one or two of the spatial dimensions can be reconstructed using data that are present and well sampled in the other spatial dimensions. This idea is to put the trace in the correct grid position and then the interpolation will fill up the holes in each offset class.

For quantity of the data, the old seismic parameter has an inline step every two, 25 m each inline, sample interval 2ms with the number of samples per trace is 1500. While the new repro has an inline step 12.5m each inline, sample interval 1ms with the number of samples per trace is 3073, Table 02.

Parameter	OLD	REPRO
Inline step	2	1
Inline interval	25m	12.5m
Sample interval	2ms	1ms
Number of sample per trace	1500	3073

Table 02. New parameter of seismic reprocessing

The final stack result from the reprocessing data qualitatively supplies a better seismic image continuity, makes it easy to interpret the horizon from the 0ms to the basement event, and clear from multiple effects (Figure 02). The spectrum frequencies are more stable, with no low and high frequencies noise at this seismic section. Another QC comes from the time slice result, new repro data showing the good image at closure boundaries in the reservoir zone (Gita) at 1000ms and in the basement zone at 1200ms (Figure 03).

Seismic Amplitude

Seismic amplitude right now is one of the important criteria for recognizing potential hydrocarbon reserves. Recognize and validating an amplitude is the key to bridging between the seismic to lithology and pore-fluid saturation (Hilterman, 2001). Amplitude interpretation must be geologically consistent with the structural analysis. In exploitation perspective, seismic amplitude data is the easiest way to characterize and identify the potential of subsurface reservoirs. An integrated and comprehensive geophysical analysis are needed to support this issue. It started by performing a running seismic amplitude attribute as the first step for an integrated geophysics study. This research will focus on the Gita Member area in the reservoir zone of Gita sand (30-1) TAF.

A seismic attribute is a quantitative measure of a seismic characteristic of interest (Chopra and Marfurt, 2005). Post stack seismic attribute are applied in seismic interpretation data to identify the anomaly, like bright spots effects, frequency anomalies, faults-structural mapping, reveal detail reservoir channels, highlight reservoir trends, and enhance technical presentation. Seismic attribute analysis begins by choosing attributes that are appropriate for the purpose at hand. Certain attributes prove to be most successful for certain objectives. Seismic attributes are cleared when derived from clean seismic data (Barnes, 2016).

To check the quality of seismic amplitude of the new repro data, we try to slice the amplitude attribute map at the Gita horizon. It provides a higher resolution image than the original post stack data. It is due to the new repro data has more inline data every 12.5m compared to the old data that only has 25m inline spacing. The 30-1 meander channel looks better resolution and more continuous compared to the old data. See the black arrows at several places (Figure 03). The yellow color indicates that the

preserve bright amplitude is likely a direct hydrocarbon indicator. The partial angle stack also being used for the QC process, which includes near data (0°-16°), mid data (16°-26°), far data (26°-36°), and ultra-far data (36°-46°). The AVO response (yellow circle) appears increasingly bright from near to ultra-far seismic data (Figure 04), it shown in the slicing attribute amplitude data (Figure 05).

Rock Physics

Seismic data analysis is one of the keys methods for reservoirs characterization and monitoring subsurface pore fluids. While there have been greats advances in 3D seismic data processing, the quantitative interpretation of the seismic data for rock properties still poses many challenges. Quantitative seismic interpretations demonstrate how rock physics can applying to predict reservoir parameters, such as lithologies and pore fluids, from seismically derived attributes (Avseth, et al., 2005).

One of the primary goals of amplitude interpretation is to determine whether a water-saturated rock or a hydrocarbon-saturated rock. (Hilterman, 2001) Thus, a few basics relationships of rock physics are necessary. Before running seismic inversion, it is important to understand the relationship between reservoir properties, seismic amplitudes and also the petrophysical data of the different rock physics.

The first procedure in starting rock physics analysis is to conduct a feasibility study through the cross-plot wells data with various elastic parameters. In this feasibility study, we use tens exploration wells in the Intan area. From those 10 wells, only Laras-01 has an original Vs log. A blind test well was tested on Laras-01 well to figure out how confident the Vs prediction would be for all wells (Figure 06). The procedure for predict Vs log in this study is using Modified Gassmann (sandstone reservoir) while if the calculation was failed, then Greenberg Castagna was applied to the data. The results of the blind test well produce data Vs predictions, which qualitatively look very good compared to the original Vs data log, shown by the cross plot of Vs predicted vs Vs measured and also AI vs Vp/Vs on the Laras-01 well.

This Vs log prediction using those methods then applied to all wells. After that process, a fluid replacement model (FRM) is applied to the cross-plot data. The petro elastic behavior cross plot at 100% Sw showed that the lithology of wet sand, shale, and coal could be well separated. From petro elastic behavior at in situ conditions, we can see that oil saturation can be separated clearly from the wet sand. Low VpVs ratio values and low saturation density indicate the characteristics of hydrocarbon oil. A cross-plot matrix on the INTA-01 well made to figure out which of the best elastic properties parameters to characterize the reservoir.

From the cross-plot results, we obtained several elastic parameters that can characterize the reservoir, such as AI vs VpVs ratio and Lambda-Rho (LR) vs Mu-Rho (MR) with a cut-off VpVs ratio below 2 for oil sand and LR below 15 GPa*g/cc (Figure 07). The AI and SI values in the cross-plot data cannot separate well between sand and shale lithology. It is necessary to try another method like Poisson's Impedance (PI) for solving this issue. (Direzza, et al., 2012) tweaking these methods by varying the C value and dividing it into two categories, namely Lithology Impedance (LI) and Fluid Impedance (FI). We apply using this method at Intan-01 well.

LI is obtained from the correlation coefficient between PI and Vclay, while FI is from the PI and Sw. The maximum values for C on the LI and FI are 1,475 and 1,525 based on the results of the Target Coefficient Correlation Analysis (TCCA) curve as seen from (Figure 08). Then that formula is applying to all the well to see the cut off value of LI and FI. It shows that oil sand, wet sand, and shale can be separated with cut off values for oil sands below 5000 ft/s*g/cc.

AVO Attribute Volume

Since 1970, the bright spot era in seismic data has become a favorite as a powerful tool for direct indicators of the presence of a hydrocarbon. It did not take long to realize that not all hydrocarbon reservoirs were bright. Dim out effects also have the same response as an indicator for hydrocarbons. In 1984, 12 years after the bright spot technology became a commercial tool for hydrocarbon prediction, Ostrander published a breakthrough paper (Ostrander, 1984). He showed that the gas presence in sandstone reservoir capped by a shale would cause an amplitude variation with offset (AVO) in pre-stack seismic data. Then, (Shuey, 1985) confirmed mathematically via approximations of the Zoeppritz equations that Poisson's Ratio was the elastic constant most directly related to the offset-dependent reflectivity for incident angles up to 30°. AVO technology, a commercial tool for the oil industry, was born (Avseth, et al., 2005).

After that, the era of AVO analysis, AVO mapping, and cross-plot data rapidly developed until the end of the '90s. By sequential, (Smith & Gidlow, 1987) with fluid factor analysis, (Rutherford & Williams, 1989) with three AVO classes, (Fatti, et al.,1994) with the fluid factor in term of Vp &Vs, (Castagna & Swan 1997) with intercept and gradient cross plot and then (Goodway, et al., 1997) with the Lambda-Mu-Rho analysis makes AVO is powerful tools for oil hydrocarbon detection. AVO method application in the Intan field was first carried out by (Harmoni, et al., 1996). The purpose of this study is to determine the Intercept (P), Gradient (G), (P * G), and AVO far offset (AVO30 °) to have a better understanding of the AVO response. The impedance value of the sand and carbonaceous shale mapped and separated well. It will make it easier to re-evaluate and review the proposed infill well prospects.

The earlier discussion in (Figure 04) and (Figure 05), shows that the amplitude map in the near, mid, and far data indicating AVO response with an amplitude gets brighter as the offset increases. There is an anomaly bright spot effect that indicated the presence of hydrocarbons. Intercept (P) volume, Gradient (G) volume, Fluid Factor (F), and P*G volume are obtained by deriving them from the angle stack data (Figure 09).

AVO curve analysis at the PSTM gathers data near INTA-01 well shown that there is a strong anomaly amplitude with increasing offset. These can see from the increasing curve magnitude of the analysis on the far offset

data (Figure 10). Whereas in the Susana-01 well, the PSTM gather is flat, with no AVO response, which indicates that there is no hydrocarbon in the well.

Simultaneous Inversion

In line with the AVO growing era, several scientists have succeeded in developing the seismic inversion method. (Connoly, 1999) have succeeded in developing the seismic inversion method with elastic parameters, (Ma, 2001) with the Simultaneous / AVO inversion method and (Whitcombe, et al., 2002) with the Extended Elastic Inversion (EEI) method to complement and develop the acoustic inversion method that has established since (Lindseth, 1979) first introduced it.

Prestack inversion can be used to extract both compression and shear information from P-wave acquisition. It also can be useful in DHI for both carbonate and clastic rocks, and it can be significant to derive elastic rock properties and quick determination for fluid and lithology discrimination of reservoirs (Goodway, et al, 1997; Gray & Andersen, 2000).

Reservoir characterization requires the identification, detection, quantification of thickness, permeability, porosity, and also fluid content. But unfortunately, many of these reservoir parameters are not directly derivable from seismic data. AI and SI estimated using the simultaneous inversion scheme can be used to derive the conventional rock properties such as Vp/Vs or Poisson's ratio (Ma, 2001).

Before performing the pre-stack inversion process on this data, first, we tried to see the relative impedance attribute as an initial screening of the inversion response. Estimated relative AI is calculated by integrating the seismic trace, and then passing the result through a high-pass Butterworth filter. When the extract value amplitude at this relative impedance is compared to the seismic original data, it is clear that the impedance is adequate to describe reservoir 30-1. Low AI values are associated with bright amplitude in the seismic section.

The angle stack data (near, mid, and far) from new seismic reprocessing data are used to build the simultaneous inversion model. The wavelet extracted in each volume. Using common workflow for simultaneous inversion, qualitatively the training data (Vp, Vs, Rho, and Vp/Vs) compared to the input data is quite good. Correlation between synthetic and seismic data at INTA-01 well is 0.96 from window 960ms to end of log (1060ms) while error between synthetic and seismic data is 0.27.

(Figure 11) shows the results of the simultaneous inversion that produces AI, SI, Rho, and Vp/Vs volumes. With these multiple output volumes, another elastic parameter such as Poisson's Ratio (PR), LR-MR, Lambda/Mu (L/M), LI, and FI can be derived mathematically. The analysis of all these attributes shows the consistency of the oil sand presence (indicated by the red polygon area). It is suitable with the rock physics matrix cross-plot, with low AI, low LR, low Vp/Vs ratio, low L/M, low PR, and low LI-FI values. That area is structurally high, especially near to the INTA-01 well.

Seismic Lithology and Fluid Detection

With a good quality of seismic data from seismic reprocessing, it's now easy to quantify and predict lithology and fluid contents. It was imperative to combine deterministic physical models with geostatistical techniques. This method is fundamental for estimate reservoir rock properties derived from seismic data. (Avseth, et al. 2005) explain this procedure by identifying the most likely interpretational, the uncertainty, and then guide the quantitative decision analysis. (Buland & More, 2003) defined a new linearized AVO inversion technique to obtain posterior distributions for Vp, Vs, and density that developed in a Bayesian framework.

In this study, we want to quantify uncertainty in seismic by dividing with the lithology and fluid prediction. By using several elastic parameters from seismic inversion data, this method is based on a supervised Bayesian classification to deliver several probability cubes of predicted rock properties or lithology. The integrated workflow will give us a good understanding of lithology classes. It can also predict a more accurate assessment of fluids and lithology probabilities.

For this project, we just use LR-MR data from simultaneous inversion as an input. As shown in the cross plot (Figure 12), the facies classification has divided into three classes (sand, shale, and coal) and four classes (oil sand, wet sand, shale, and coal). The probability density function cross plot result is applied to the seismic data to obtain the probability volume of each facies. Then it converts to the seismic lithology volume and the seismic fluid volume.

The oil zone (at the red polygon area) in (Figure 13) also shows the same consistency as the other elastic attributes. Indicating that OWC can be justified using this interpretation. The slice results in the 30-1 reservoir zone show that the lithology of sand and shale can be mapped easily, especially with carbonaceous shale-coal in the Yayuk-01 and Susana-01 wells, which cannot distinguish on the AI map and amplitude attribute map. This result is consistent with what (Harmoni, et al., 1996) study done. VpVs ratio map and the Lambda-Mu (LM) map, near the area of that well (Susana-01 and Yayuk-01), also have high VpVs and LM values.

Spectral Decomposition

Spectral decomposition provides a novel means of utilizing seismic data for mapping temporal bed thickness, imaging, and geologic discontinuities over larges 3D seismic surveys. (Partyka, et al., 1999). He introduces spectral decomposition to the industry at large. Oil and gas reservoirs can cause anomalies in the energy and frequency of seismic signals. Strong amplitude anomalies at specifics frequencies have been found easily by using spectral decomposition.

In this study, CWT (Continuous Wavelet Transform) has been applied to the 3D full-stack seismic data to understand the character of a reservoir compared to conventional seismic data. After decomposing the 3D seismic data, several frequencies were gathered from 10-90Hz. 30-1 reservoir images can be identifying starting at 33 Hz frequencies. This CWT seismic data shows good images identifying the hydrocarbon anomalies indicated by

the red circle polygon compared to the legacy seismic data (Figure 14). The bright amplitude anomaly response in the INTA-01 well was not visible in the Yayuk-01 and Susana-01 wells. Both wells have no reservoir and hydrocarbon because its carbonaceous shale (yellow circle) (Figure 14).

Animation through discrete spectral decomposition images helped interpreters understand the stratigraphic setup of this potential reservoir. One of the most common color image techniques is to plot three discrete frequencies against red, green, and blue (RGB) (Chopra & Marfurt, 2005). In this study, three partial stack data at near-mid-far and three spectral components 41 Hz, 56 Hz, and 70 Hz against RGB are plotted (Figure 15). Hydrocarbon anomalies can be seen clearly by applying this RGB blending method from these two data sets. Red color anomalies at near-mid-far, indicating strong amplitude response/AVO anomaly at far offset data. For CWT images, cyan color (high frequency) interpreted to levee complexes. While magenta and yellow indicating the thickest channels and dark colors indicating low reflectivity.

Result and Discussion

Seismic repro data can provide better results than the legacy data, especially in 30-1 reservoir slicing amplitude. The reflector continuity looks acceptable, and the amplitude, frequency, and phase are maintained in preserved condition. There is no issue about multiple and reverberation again since it can be eliminated very well using predictive Tau-Pi deconvolution and radon demultiple. Regularization and interpolation also helpful to fill up the empty trace and set the best full fold coverage.

The AVO analysis on the angle stack data shows that the amplitude value from near to far data is getting bright with the increasing offset. This anomaly also can be seen in the PSTM gather, near the INTA-01 well, which shows the AVO curve, indicates the hydrocarbon presence. While near Yayuk-01 and Susana-01 show flat responses, indicating the absence of hydrocarbon.

Feasibility cross plot results from rock physics analysis show that the sandstone reservoir can be separated very well, especially on Vp/Vs and LR-MR data. Another method tested by using Poisson Impedance since it is difficult to distinguish between AI and SI values in a cross plot. Correlation results between Lithology Impedance (Vclay) and Fluid Impedance (Sw) look favorable.

Lithology and fluid classification using the Bayessian method applied to LR-MR data from the seismic prestack inversion. It gives tremendous results, detecting lithology and hydrocarbon fluid presence. This method successfully identified the ambiguity between lithology sand and carbonaceous shale, also the HC content. The oil sand area has consistent trends compared to other methods.

Apart from the amplitude side, the frequency side of the data was also analyze using spectral decomposition. The oil sand area has an amplitude magnitude that looks brighter. Finally, the RGB blend was tested using three data sets (near-mid-far) and spectral decomposition data sets (41-56-70Hz). The RGB blend looks perspicuously, and when integrated with other methods, it will strengthen the presence of hydrocarbons and lithologies.

Conclusions

With the evolution of the computer technology era and sophisticated seismic processing techniques, hydrocarbon fluids identification and the quantification approach can be easier to execute. 3D seismic reprocessing data is an absolute prerequisite that is currently needed. Qualitatively and quantitatively, these new seismic data look better compared to the previous data. The proposed workflow can simplify the interpretation, better understand the reservoir character, and reduce uncertainty risks by integrating practical techniques.

Several attributes like seismic partial/angle stack, Intercept-Gradient AVO, Fluid Factor, Lambda-Rho Mu-Rho, lithology impedance, litho-fluid detection, seismic facies, and spectral decomposition tested on a 30-1 reservoir. It exhibited tremendous results detecting the presence of hydrocarbons in the Intan field. The OWC of this reservoir can be determined and clearly by integrating the results of this study. It will make a greats impact as an input of the static model in the future step process.

Several types of opportunities were obtained within this seismic QI feasibility study, as follow:

1. Improve communication within the working team, management, or another stakeholder about deliverability and expectations. It could reduce failure chances because of miscommunication and or different expectations between the stakeholders.
2. Provide alternative scenarios or multiple possible solutions to anticipate changes because of the current data, information, technique boundaries to maintain the project completed promptly.
3. Provide credibility because whatever we are doing is systematic, non-random, measurable, and repeatable.

Acknowledgements

We would like to thank Pertamina Hulu Energi OSES and SKK Migas for providing permission and the proprietary data information for this study, Asri Basin working team was instrumental in defining the path of our research, also for Advisors in Pertamina for guidance through each stage of the process. We would also very grateful to acknowledge the Pusat Studi Energi UGM for providing the new reprocessing seismic data and for inspiring our interest in the development of innovative technologies.

References

Aldrich, J.B., Rinehart, G.P., Susandhi, R., Schuepbach, M.A., 1995. Paleogene Basin Architecture of the Sunda and Asri Basins, and Associated Non-Marine Sequence Stratigraphy, Proceedings, International Symposium on Sequence Stratigraphy in SE Asia, p. 261-287.

Avseth, P., Mukerji, T., Mavko, G., 2005. Quantitative Seismic Interpretation: Applying Rock Physics Tools to Reduce Interpretation Risk. Cambridge Univ. Press.

Barnes, A.E., 2016. Handbook of Poststack Seismic Attributes. SEG Library. Geophysical References Volume **21**.

Buland, A., Omre, H., 2003. Bayesian linearized AVO inversion. Geophysics **68**, 185–198.

Castagna, J.P., Swan, H.W., 1997. Principles of AVO crossplotting. Lead. Edge **16**, 337–344.

Chopra, S., Marfurt, K.J., 2005. Seismic attributes-A historical perspective. Geophysics **70**, 3SO-28SO.

Connolly, P., 1999. Elastic impedance. Lead. Edge 18, 438–452.

Direzza, A., Permana, I., 2012. The Application of Poisson Impedance Inversion for Sandstone Reservoir Characterization in the Lower Talang Akar Formation, Case Study Melandong-West Java. AAPG International Comference & Exhibition.

Fatti, J.L., Smith, G.C., Vail, P.J., Strauss, P.J., Levitt, P.R., 1994. Detection of gas in sandstone reservoirs using AVO analysis: a 3-D seismic case history using the Geostack technique. Geophysics **59**, 1362–1376.

Goodway, B., Chen, T., Downton, J., 1997. Improved AVO fluid detection and lithology discrimination using Lamé petrophysical parameters; "λρ", "μρ", & "λ/μ fluid stack", from P and S inversions, in: SEG Technical Program Expanded Abstracts 1997. Society of Exploration Geophysicists, pp. 183–186.

Gray, D., Andersen, E., 2000, Application of AVO and inversion to formation properties: World Oil, **221**, July, 85-90.

Harmony, W. E., Gilmore, H.L., Armon, J.W., Smith, S. W., Danahey, L., Himawan, R., Bowman, T. L., Smith, W., 1996. An example of 3-D AVO for lithology discrimination in Widuri Field, Asri Basin, Indonesia. The Leading Edge. SEG Library.

Hilterman, F.J., 2001. Seismic amplitude interpretation. (Society of Exploration Geophysicists and European Association of Geoscientists and Engineers).

Lindseth, R.O., 1979. Synthetic sonic logs—a process for stratigraphic interpretation. Geophysics **44**, 3–26.

Ma, X.-Q., 2001. Global joint inversion for the estimation of acoustic and shear impedances from AVO derived P- and S-wave reflectivity data. First Break **19**, 557–566.

Ostrander, Wj, 1984. Plane-wave reflection coefficients for gas sands at non-normal angles of incidence. Geophysics 49, 1637–1648.

Partyka, G., Gridley, J. and Lopez, J. (1999) Interpretational Applications of Spectral Decomposition in Reservoir Characterization. The Leading Edge, **18**, 353-360

Rutherford, S.R., Williams, R.H., 1989. Amplitude-versus-offset variations in gas sands. Geophysics **54**, 680–688.

Sheriff, R.E., Geldart, L.P., Telford, W.M., 1992. Applied Geophysics Second Edition. Cambridge university press.

Shuey, R.T., 1985. A Simplification of the Zoeppritz equations. Geophysics **50**, 609–614.

Smith, G.C., Gidlow, P.M., 1987. Weighted stacking for rock property estimation and detection of gas. Geophys. Prospect. **35**, 993–1014.

Sukanto, J., Nunuk, F., Aldrich, J. B., Rinehart, G. P., Mitchell, J., 1998. Petroleum System of The Asri Basin Java Sea Indonesia. Proceeding IPA 26th Annual Convention.

Whitcombe, D.N., Connolly, P.A., Reagan, R.L., Redshaw, T.C., 2002. Extended elastic impedance for fluid and lithology prediction. Geophysics **67**, 63–67.

Wight, A., Friestad H., Anderson, I., Wicaksono, P., Reminton, C.H., 1997. Exploration history of the offshore Southeast Sumatra PSC, Java Sea, Indonesia. Geological Society, London, Special Publications, **126**, 121-142.

Young, R., Atkinson, C.D., 1993. A Review of Talang Akar Formation (Oligo-Miocene) Reservoirs in the Offshore Areas of Southeast Sumatra and Northwest Java, in Clastic Core Workshop, Special Publication of the IPA.,pp. 177-210.

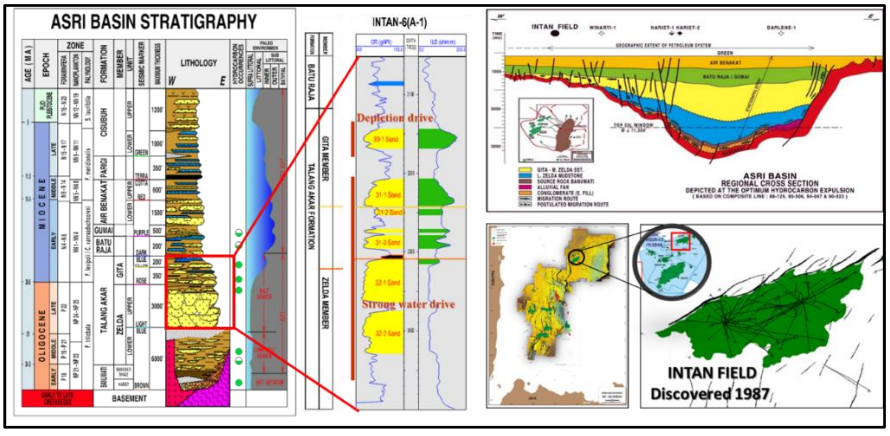

Figure 01. Asri Basin stratigraphy, log type and regional cross section

No	LEGACY DATA (1991)	No	REPROCESSING (2020)
1	Reformat	1	Reformat Field Data to internal format
2	Anti Aliasing Filter	2	3D Geometry & navigation (Bin Size 12.5M x 12.5M)
3	Resample 2ms	3	Designature Minimum Phase
4	Dephasing Filter	4	Gun & Cable Static Correction
5	Spherical Divergence	5	Low cut filter apply
6	Surface Consistent Deconvolution	6	Bad Trace or denoising
7	CMP Gather	7	Swell Noise Removal & Coherence noise removal
8	Veocity Analysis Every 1km	8	Direct Arrival Noise Removal & Linear Noise removal
9	Static Binning 6.25m x 25m	9	Spherical divergence correction
10	Dip Move Out (DMO) Finite Difference	10	Regional velocity analysis every 1km
11	Velocity Analyses Every 0.5km	11	3D SRME or Shallow water demultiple
12	Flexible Binning using 15% bin overlap	12	Shot and cable compensation
13	Normal Move Out (NMO) mute	13	Tau-P Deconvolution
14	Multigate Scaling	14	Denoising
15	Partial Stack	15	1st velocity analysis every 500m X 500m
16	Final Stack	16	High Resolution Radon Demultiple
17	Adjacent Trace Sum in ILINE Direction	17	Residual Noise Attenuation
18	5 Trace Lateral Normalization	18	Regularization & 5D Interpolation
19	Trace Interpolation in XLINE Direction	19	Footprint removal
20	One Pass Migration Based on Finite Diference	20	Residual Shallow water demultiple (if Required)
21	Band Pass Filter	21	3D PSTM for velocity analysis Every 250m X 250m
22	Dynamic Trace Equalization AGC	22	3D Full Kirchhoff PSTM
23	Film Display	23	Final Velocity Picking Every 250m X 250m
		24	High Resolution Radon Demultiple
		25	Output PSTM Gather in SEGY Format
		26	Normal moveout correction (NMO) and Mute
		27	Output Raw PSTM Stack in SEGY Format
		28	Zero Phase Conversion
		29	Random Noise Attenuation
		30	Time variant filter & Time Variant Scaling
		31	Output Filtered & Scaling PSTM Stack in SEGY
		32	SEG-Y Angle Stack (Near, Mid and Far Angle Stack)
		33	Output PSTM Velocity

Table 01. Legacy Data (1991 processing) and New Processing Flow (2020)

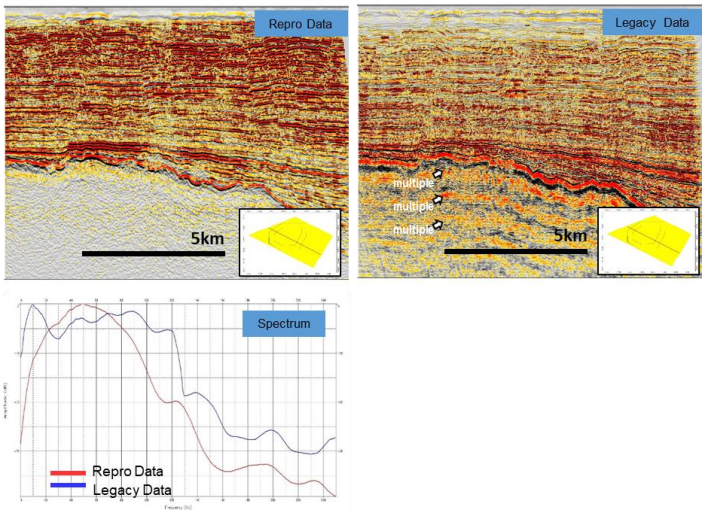

Figure 02. New reprocessing data (left) compared to legacy seismic 1991 data (right). Looks like the S/N ratio improve, less multiple effect, and good continuity reflector at several even. Spectrum from the repro data looks more stable, there is no low and high frequencies noise at this final data stack.

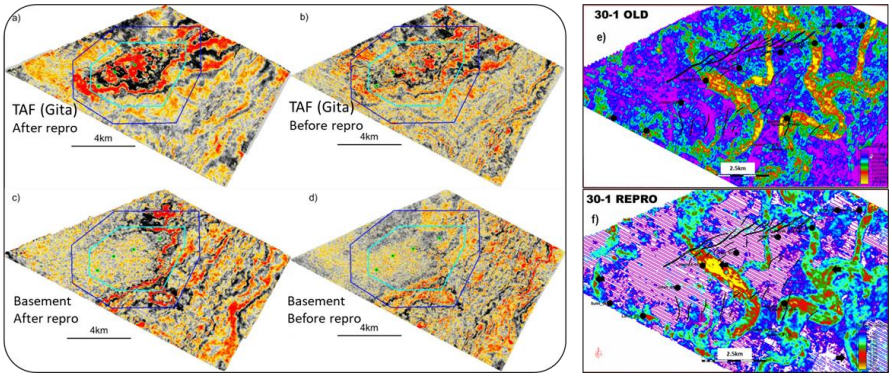

Figure 03. Time slice at 1000ms (near Gita reservoir zone) and at 1200ms (near basement) showing good result and continuity from a) & c) repro data compare to b) & d) legacy seismic data. Horizon slices at 30-1 reservoir showing meandering channel. f) Reprocessing seismic data showing good image result and continuity (black arrows) compared to e) legacy seismic data.

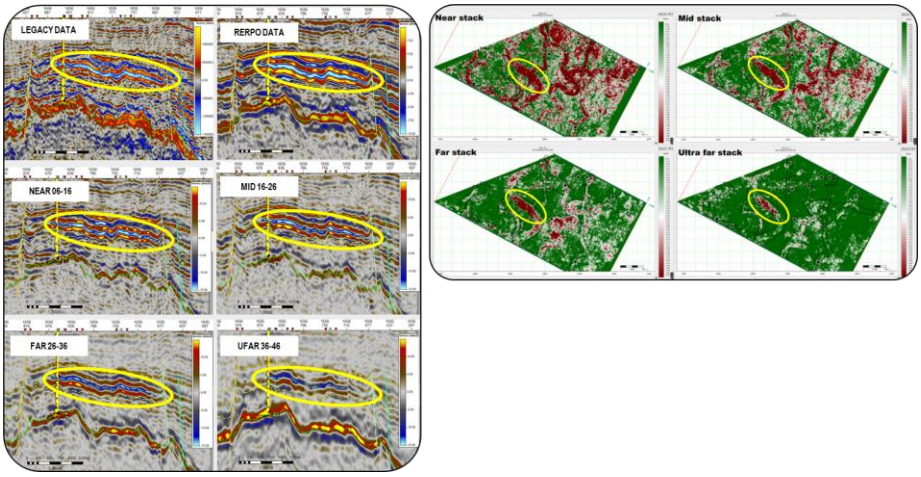

Figure 04. Angle stack data showing the AVO anomaly effect on 30-1 reservoir (yellow circle). The amplitude is getting bright as increasing the angle/offset. Figure 05. Horizon slice on angle stack data showing the AVO anomaly effect on 30-1 reservoir.

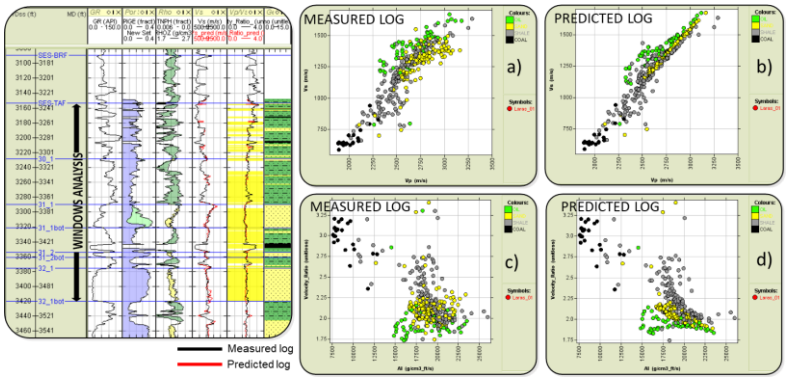

Figure 06. Blind test well on Laras-01 to predict Vs log, predicted log (red curve) qualitatively relative match with the measured log (black curve). Cross plot Vp vs Vs at measured log (a), predicted log (b) and cross plot AI vs VpVs ratio at measured log (c), predicted log (d)

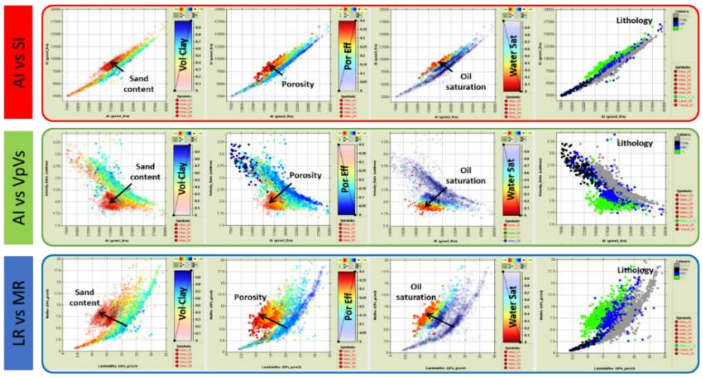

Figure 07. AI vs SI, AI vs VpVs and Lambda-Rho vs Mu-Rho at various color key (Vclay, porosity, lithology, and Sw). From these crossplot analysis, Vp/Vs ratio and LR can distinguish between reservoir and non-reservoir.

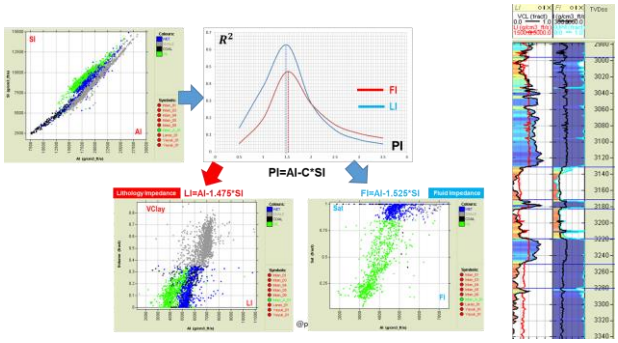

Figure 08. TCCA for Lithology Impedance (corelate with Vclay) and Fluid Impedance (corelate with Sw) at Intan-01 well. The cut off for oil sand is below 5000 ft/s*gr/cc.

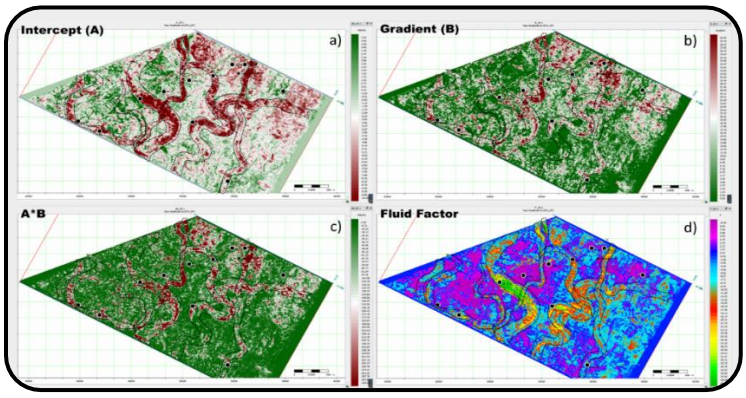

Figure 09. AVO Attribute map a) Intercept (A), b) Gradient (B), c) Product A*B, d) Fluid Factor

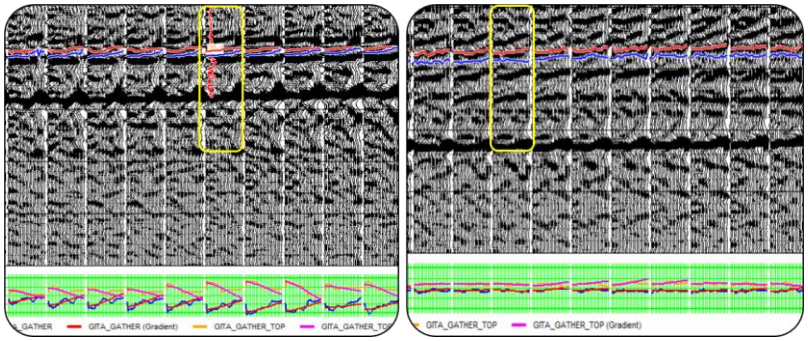

Figure 10. AVO response curve analysis from INTA-01 (left) at 30-1 reservoir showing the anomaly at far offset, while Susana-01 (right) showing flat AVO curve indicating that there is no hydrocarbon at that area.

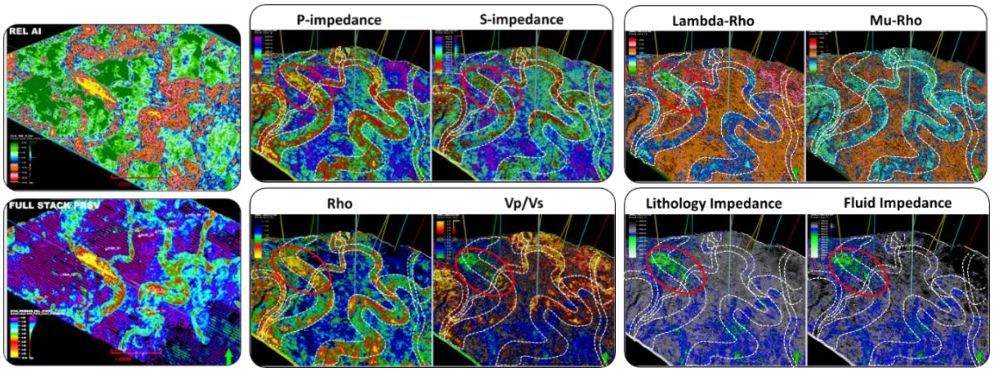

Figure 11. Relative impedance attributes at 30-1 reservoir using low cut frequency 10 Hz compared to original 3D preserve full stack seismic amplitude and Simultaneous Inversion map (AI, SI, Rho, and VpVs Ratio). The hydrocarbon anomaly (red circle) indicated by low value of AI, LR, Vp/Vs, LI, and FI.

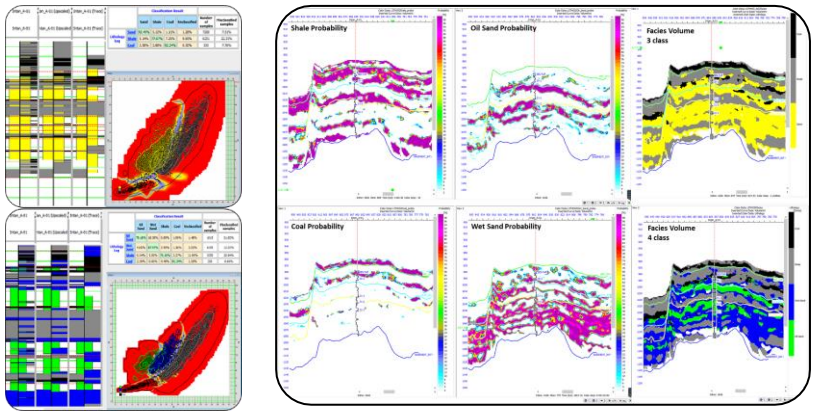

Figure 12. Lithology classification using PDF at 3 classes (Sand, Shale, Coal) and 4 classes (Oil Sand, Wet Sand, Shale, Coal). Probability volume from oil sand, wet sand, coal, and shale based on Bayesian classification.

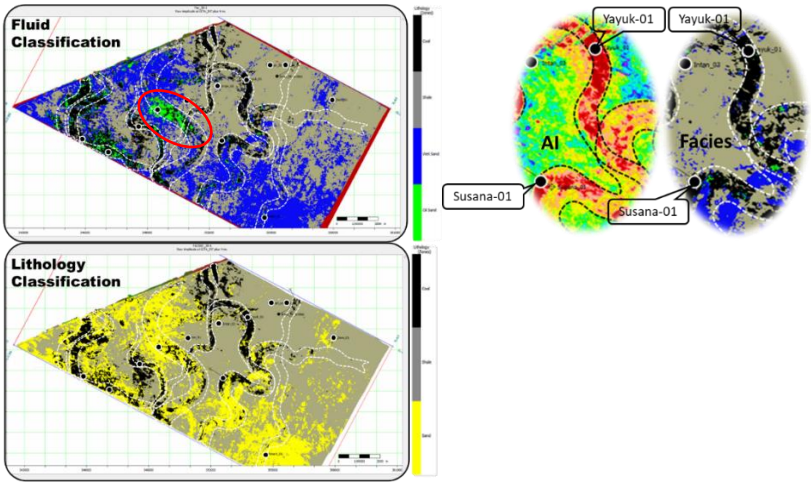

Figure 13. Lithology and Fluid classification map at 30-1 reservoir showing oil sand (green color) accumulated at red ellipse polygon. AI Attribute cannot distinguish between sand and carbonaceous shale, while facies attribute derived from Bayesian classification successfully separate between sand and carbonaceous shale.

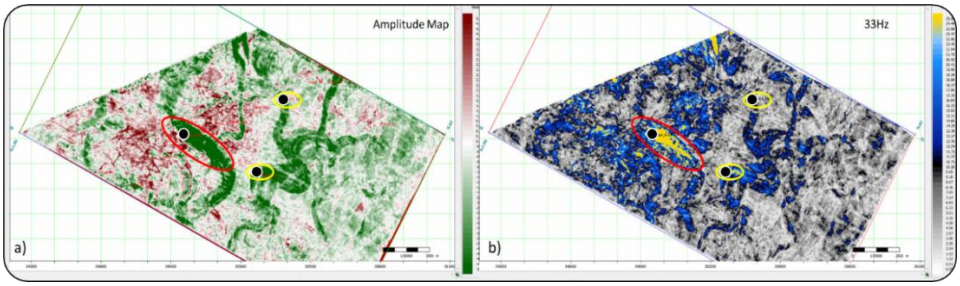

Figure 14. 30-1 CWT attribute map showing high amplitude anomalies (red circle) near INTA-01 well, while the dim amplitude (yellow circle) near the Yayuk-01 and Susana-01 indicating absences of hydrocarbon.

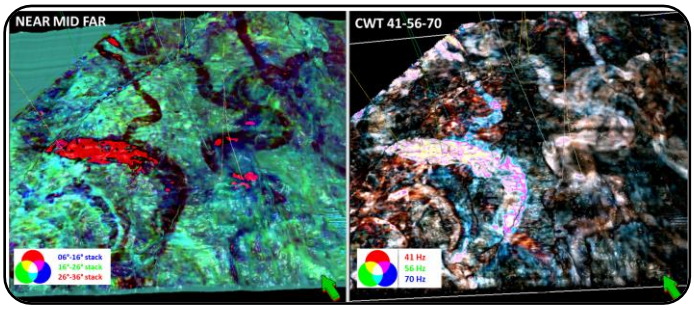

Figure 15. RGB blend at partial stack (left) and CWT map (right) at 30-1 reservoir. Red color anomalies at near-mid-far, indicating strong amplitude response/AVO anomaly at far offset data. For CWT images, cyan color (high frequency) interpreted to levee complexes. While magenta and yellow indicating the thickest channels and dark colors indicating low reflectivity.